Applied Food Research 6 (2026) 101717

Contents lists available at ScienceDirect

Applied Food Research

journal homepage: www.elsevier.com/locate/afres

Smart eco-friendly packaging for spoilage detection of fresh chicken, salmon, and shrimp products

Ludovica Milzi [a], Rosita Diana [a,*], Francesco Silvio Gentile [b], Pasquale Ferranti [a], Ugo Caruso [b], Fabio Mazzaglia [c], Barbara Panunzi [a]

[a] Department of Agriculture, University of Napoli Federico II, Reggia di Portici - Piazza Carlo di Borbone, 1 80055, Portici (NA), Italy
[b] Department of Chemical Sciences, University of Napoli Federico II, Strada Comunale Cinthia, 26, Napoli 80126, Italy
[c] C.R.A. S.r.l., Calle Giovanni Legrenzi, 2, VE, Venice 30171, Italy

A R T I C L E I N F O

Keywords:
Smart packaging
Food spoilage
Colorimetric sensor
VOCs
SEM
GC

A B S T R A C T

At the consumer level, labels for in-situ monitoring by the naked eye are useful tools as indicators of food freshness. Smart labels are often pH-sensitive and reactive to volatile bases. Expanding their response range to various food spoilage VOCs can improve performance and applications. In this study, we aimed to develop an innovative, easy-to-assemble, and multi-reactive colorimetric label based on environmentally friendly and cost-effective ingredients. The label was produced by layer-by-layer deposition of PVA, pectin, and copper (II) gluconate within preformed commercial polystyrene trays for food packaging. The copper salt, commonly used in dietary supplements, serves as the sensing compound, while the pectin host matrix acts as a carrier, forming a hydrogel that allows interaction with volatile analytes. The label provides a colorimetric response in the presence of various N- and S-based VOCs produced during the spoilage of protein foods (salmon, shrimp, and chicken) at storage conditions of 4 °C and 25 °C. To investigate the mechanism, we collected data on the interaction of copper (II) gluconate with ammonia, trimethylamine, hydrogen sulfide, and thiols, and attributed the colorimetric response to various coordination, redox, and precipitation reactions. A representative model of the salt response was obtained through theoretical calculations. The labels used were analyzed by scanning electron microscopy and gas chromatography, attempting to correlate the N- and S-based VOC profile with the colorimetric response. Ease of production, eco-sustainability, and low-temperature efficacy combine with the convenience of monitoring food preservation via color management software on a common smartphone.

1. Introduction

The food industry is called to satisfy consumers' increased demand for safe, nutritious, healthy food. Among these requirements, food safety and integrity have always been the primary public concern due to their deep impact on the population's health and welfare (Fan, Rakotondrabe, Chen, & Guo, 2023). Related to the aspects of quality and safety, the cheap and on-site evaluation of the freshness of a food product is one of the most desirable goals for either industry or consumers (Milzi, Diana, & Panunzi, 2025; Zhao, Liu, Zhao, & Wang, 2022).

Food spoilage and deterioration are naturally occurring processes affected by various factors, such as microorganisms, air, light, temperature, and time (I. N. Ashie, Smith, & Simpson, 1996). Visual appearance, texture, flavor, and taste are common indicators used to assess food quality and safety changes. Volatile organic compounds (VOCs) are composed of various classes of compounds volatile at room temperature (vapor pressure ≥10 Pa at 20 °C) that contribute to the unique aroma fingerprint of each food type; they include aldehydes, ketones, alcohols, aromatic compounds, sulfur compounds, amines, esters, and acids (Feng, Wang, Beykal, Qiao, Xiao, & Luo, 2024; Li, Pal, & Kannan, 2021). Food ageing leads to changes in the VOC profile. VOCs released during food spoilage processes may act as the signature of a particular state of storage. Nowadays, VOCs are used as biomarkers for diagnosis and quality management in various fields of application, including food (R. Diana et al., 2024; Tiwari et al., 2020). However, the quantitative analysis of VOCs released from foods in general requires sophisticated, time-requiring, and expensive technology, such as an electronic nose and GC-MS (Delgado-Rodríguez, Ruiz-Montoya, Giraldez, López, Madejón, & Díaz, 2012). On the other hand, rapid analysis and portable equipment are essential for food safety, hence the growing demand for

* Corresponding author.
E-mail address: rosita.diana@unina.it (R. Diana).

https://doi.org/10.1016/j.afres.2026.101717
Received 25 June 2025; Received in revised form 28 December 2025; Accepted 20 January 2026
Available online 21 January 2026

intelligent detection systems particularly during long-term storage (Perez de Vargas-Sansalvador, Erenas, Martínez-Olmos, Mirza-Montoro, Diamond, & Capitan-Vallvey, 2020; Ye, Li, Xie, & Wu, 2022)

Intelligent packaging is one of the novel packaging technologies, including different materials, instruments, and technologies (Kalpana, Priyadarshini, Maria Leena, Moses, & Anandharamakrishnan, 2019) to monitor food products. Naked-eye in-situ responsive labels are expanding researchers' interests for their low cost in operation and assembly, ease, and non-invasiveness. Based on VOCs detection, colorimetric indicators of the total volatile basic nitrogen compounds (TVB-Ns, such as ammonia, dimethylamine, and trimethylamine) are the most common tools for monitoring food freshness (Balbinot-Alfaro, Craveiro, Lima, Costa, Lopes, & Prentice, 2019). Some colorimetric indicators do not need to be in direct contact with food to monitor the quality and can be applied between packaging layers (Silva et al., 2024). When the colorimetric signal is due to the contact between the food and the indicator, synthetic functional dyes have limited applications (Bhargava, Sharanagat, Mor, & Kumar, 2020; R. Diana, Caruso, Di Costanzo, Bakayoko, & Panunzi, 2020; Lee et al., 2019; Lydekaityte & Tambo, 2020; Ma et al., 2021) while natural dyes, such as anthocyanins, has been largely described as a valid pH indicator responsive to TVB-Ns (Zhao et al., 2022). Nonetheless, VOCs of food products include a plethora of chemicals. Volatile sulfur compounds (VSCs) such as hydrogen sulfide, dimethylsulfide, and methyl mercaptan, mainly derived from cystine and methionine, have a significant role in high-protein fish and meat products (Dordevic, Capikova, Dordevic, Tremlová, Gajdács, & Kushkevych, 2023; Passafiume et al., 2023). Smart biocompatible packaging multiresponsive to different VOC components is preferable to simple pH-sensitive labels (Teymouri & Shekarchizadeh, 2022).

Copper is a transition metal essential to the proper functioning of organs and metabolic processes, the nervous and immune system, connective tissues, and blood vessels. The Cu (II) cation is responsible for complexations, precipitations, and redox reactions with significant colorimetric variations (R. Diana, Caruso, Di Costanzo, Gentile, & Panunzi, 2021). Copper gluconate ($CuGluc_2$) is the copper salt of D-gluconic acid. It is a light blue powder soluble in water, used in dietary supplements as a synergist, a dietary and nutritional supplement for foods (Nikolaou, Anastasaki, Alsubaie, Simula, Fox, & Haddleton, 2015; Yin, Fu, Lutterodt, Zhou, Antholine, & Wamer, 2012). According to the feeding practice by the FDA, copper gluconate is generally recognized as safe for use at a level not exceeding 0.005 % in the substrate, as specified in the Code of Federal Regulations (21 CFR 582.5260). This section of the U.S. Code of Federal Regulations designates copper gluconate as GRAS (Generally Recognized As Safe) for its use in drugs, feeds, and related products. The compound is known as involved in representative biological reactions (Han, Xie, & Zhou, 2024; Smith, Reed, & Hill, 1994).

Pectin is a polysaccharide present in fruits and vegetables (Roy, Priyadarshi, Łopusiewicz, Biswas, Chandel, & Rhim, 2023). The substance is marketed as a whitish powder mainly extracted from citrus and apple as an edible gelling agent. This biodegradable and environmentally friendly biopolymer can be used as the host matrix of the responsive molecule in intelligent packaging systems (Stoica et al., 2024). Due to its hydrophilicity, pectin can facilitate the adsorption of responsive substances, allowing a rapid sensory response to the target VOCs in a humid atmosphere. Poly(vinyl alcohol) (PVA) is one of the few vinyl polymers soluble in water and susceptible of ultimate biodegradation in the presence of suitable microorganisms. Environmentally compatible PVA-based materials for a wide range of applications are known (Chiellini, Corti, D'Antone, & Solaro, 2003). Many smart and active PVA-based packaging films are biodegradable materials suitable for replacing synthetic packaging and there is a vast specific literature on this topic (Abedi-Firoozjah et al., 2023; Jiang et al., 2024).

In recent years, the food packaging (FP) industry has experienced notable advancements in response to consumers' increasing demands and challenges (Perez de Vargas-Sansalvador et al., 2020; Ye et al., 2022). This has led to a shift in the role of packaging materials, which are no longer simply used as storage containers for food. They are now expected to play a more active role in extending food products' shelf life (SL), ensuring their safety, and even improving their overall quality. These developments reflect the industry's commitment to addressing consumer needs and concerns in a more comprehensive and effective manner (Reza Abedi-Firoozjah et al., 2025; R. Abedi-Firoozjah et al., 2025; Rajic, Đorđević, Tomasevic, & Djekic, 2022; Reis, 2017; Wayman & Niemann, 2021).

Today's focus on sustainability and the use of biodegradable and eco-friendly materials is a strong point of this research. In line with the recent trend towards eco-friendly systems, the substances used for the novel smart label do not increase the non-biodegradable plastic content of traditional FP. Moreover, the costs for the new intelligent tool are sustainable, as discussed in Pf.3.3.

In this research, a polymeric multilayer film was developed, where $CuGluc_2$ was immobilized on the pectin matrix and used to assemble a novel intelligent packaging tool. The colorimetric sensor named $CuGluc_2$-PEC demonstrated its ability to monitor VOCs resulting from the spoilage of various foods in commercial packaging. The intelligent packaging was obtained from a three-layer deposition, each layer made up of non-harmful ingredients and performing a specific function (Fig. 1). The colorimetric indicator is the compound $CuGluc_2$, employed as a bacteriologically pure galenic preparation commonly added to copper-based food supplements. The host matrix is pectin. This layer acts as a carrier for the active compound ($CuGluc_2$) and in the humid atmosphere produced by the food samples creates a hydrogel environment that enables interaction with the volatile analytes. The third layer made of food-grade PVA anchors the responsive part to the tray's polystyrene (PS) surface. The tool was added to preformed commercial PS trays commonly used for packaging fresh foods. An in-depth analysis of the responsive mechanisms of $CuGluc_2$-PEC was performed. Experimental data were correlated with a theoretical approach based on a model of $CuGluc_2$ in a humid environment. $CuGluc_2$-PEC label demonstrated to capture TVB-Ns and VSCs produced during spoilage of different protein-rich foods (salmon, shrimp, and chicken) at recommended (4 °C) and accelerated (25 °C) storage conditions by using RGB colour parameters. A mobile Android app based on a specific software was used to monitor colour changes of the label as a function of time. A comprehensive analysis was performed by scanning electron microscopy (SEM) technique on $CuGluc_2$-PEC samples before and after exposure to VOCs to obtain information on the morphology of the sensor surphase and the composition of the sensor layer after use ("used"). Gas chromatography (GC) was used to identify some relevant VOCs in the profile of the spoiled samples. SEM and GC data were crossed with the colorimetric response of the used labels, inferring relationships between VOCs' profile and the RGB response.

2. Materials and methods

Pectin from citrus peel, 131 ± 16 kDa, was purchased from Sigma Aldrich, Code P9135, CAS 9000-69-5, purity degree 98 %; polyvinylalcohol (PVA) M_w 31,000-50,000 was purchased from Sigma Aldrich, Code 363138, CAS 9002-89-5, purity degree 98-99 %, 99+% hydrolyzed. Low-cost food-grade guaranteed PVA was purchased from Alquera (Madrid, Spain); low-cost marketed for food use pectin was purchased from Sapore Puro (Torino, Italy). $CuGluc_2$ was a Farmalabor (Barletta, Italy) ingredient commercialised as a food-grade additive for food supplements, Cod.: 001954-004, CAS 527-09-3, purity degree 99+%.

Ethyl mercaptan was purchased from TCI Europe (Zwijndrecht, Belgium), CAS RN: 75-09-1. Triethylamine, hydrogen sulfide 0.8M in THF CAS: 7783-06-4, and ammonia 28 % aqueous solution, and all solvents were purchased from Sigma Aldrich (Milan, Italy). For the copper concentration, the ICP instrument was a 700 ICP-OES (700 Series

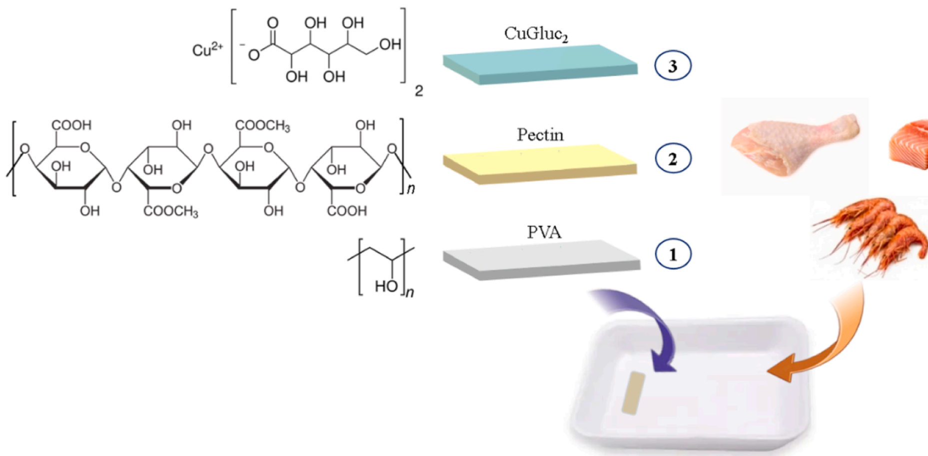

Fig. 1. Schematic representation of the components and the assembly of the detection label. In the cavity obtained in the PS tray for food use three layers were deposited in succession: PVA; pectin; copper (II) gluconate.

ICP Optical Emission Spectrometers by Agilent).

2.1. Preparation of solutions of $CuGluc_2$ for absorbance experiments

UV-visible absorption spectra were recorded by a JASCO F-530 spectrometer (scan rate 200nm/min, JASCO Inc., Easton, MD, USA) in the range 200-1000 nm. Aqueous solutions of $CuGluc_2$ $6 \cdot 10^{-3}$M (2 mL) and 1.2M of ammonia or trimethylamine (TMA) were used (5 µL aliquots). After mixing for 10 sec, the absorption spectra were recorded at room temperature.

2.2. Reaction of $CuGluc_2$ with hydrogen sulfide and with ethyl mercaptan

To 50 mL of a 0.02 M aqueous solution of $CuGluc_2$, a solution of hydrogen sulfide 0.8M in THF (1.5 mL) was added under stirring at room temperature. The precipitation of a black solid instantly ensues. The solid was recovered and washed twice with water, dried, and used for SEM elemental analysis: Cu = 62.4 % and S = 37.6 %, corresponding to CuS (theoretical analysis: Cu = 66.46 %; S = 33.54 %) black solid. Copper atom by ICP analysis: 62.0 %. Yield = 97 %.

To 50 mL of a 0.04 M aqueous solution of $CuGluc_2$, a solution of ethyl mercaptan (0.2 mL) was added under stirring at room temperature. The precipitation of a dark yellow solid instantly ensues. The solid was recovered and washed twice with water, dried, and used for further analysis for SEM elemental analysis: Cu = 54.3 %, S = 25.3 %, C = 20.4 %, corresponding to CuSEt (theoretical analysis: Cu = 50.97 %; S = 25.72 %; C = 19.27 %) yellow solid. Copper atom by ICP analysis: 51.2 %. Yield = 90 %.

2.3. Scanning electron microscopy (SEM)

SEM analyses were performed using a scanning electron microscope Thermo Phenom XL by Zeiss (Carl Zeiss NTS GmbH, Oberkochen, Germany) on the dried spun films. For the observation of the morphology of each single layer of the sensing label before and after use the operating voltage was from 5 kV to 10 kV in high vacuum (from 0.10 and 10 Pa). Magnification was set at 3800 and 8800x. For the surface elemental analysis, SEM-EDS (energy dispersive spectroscopy) technique was employed. The analysis was conducted at 10 different points for each sample and the results provided are expressed as an average. The operating voltage was from 15 kV to 10 kV in high vacuum (10 Pa). Magnification was set between 1000 and 1500x.

2.4. Headspace gas chromatography (GC)

GC was performed using 8890 GC System Gas Chromatograph coupled to 5977B Quadrupole Mass Spectrometer (Agilent). ULTRA-xr Vial Autosampler and CIA Advantage-xr Canister Autosampler connected to UNITY-xr Thermal Desorber (Markes International). To analyse the vapors produced after 5 days at 25 °C, the food samples were placed in PET airtight containers equipped with a pierceable septum. The headspace gas collected on the food samples was directly injected into the GC column. The analyses were carried out using an internationally accredited laboratory's EPA TO 15A 2019 method.

2.5. Ammonia titration

Gaseous ammonia in the vapors produced after 5 days at 25 °C was analysed according to methods 632 UNICHIM (for the gaseous phase uptake) and 4030-C APAT IRSA (for the titration) by an internationally accredited laboratory.

2.6. Assembly of the sensing tool $CuGluc_2$-PEC into the commercial PS tray

$CuGluc_2$-PEC labels were assembled layer by layer starting from a cavity obtained in the PS tray (see scheme in Fig. 1). The cavity is approximately 77 mm x 20 mm and 2mm thick. Three aqueous solutions were prepared. The solution (1) was obtained by dissolving 20 g of PVA in 10 mL of water. The solution (2) was obtained by dissolving 5 g of pectin in 50 mL of water. The solution (3) was obtained from $CuGluc_2$ 0.1 M. For each tray, 0.3 mL of the solution (1) was deposited in the cavity, and the first layer was dried in air overnight. The second layer was deposited on the PVA dried layer. For each tray, 4 mL of the solution (2) was deposited on the PVA layer and dried in air overnight. Finally, for each tray, 2 mL of the solution (3) was deposited on the dried pectin layer and dried in air overnight.

2.7. Food samples preparation

Food samples, including chicken, salmon, and shrimp, were fresh samples purchased from a local supermarket. The food samples were placed in commercial PS trays approximately 27 × 18 cm. Each tray contains one of the following samples: a fresh chicken thigh (approximately 200 g); a salmon fillet (approximately 100 g); three shrimps (for a total of approximately 150 g). The packages were wrapped in a PVC/PVDC copolymer (Saran) cling film for food use. Experiments were carried out at recommended storage conditions (4 °C) and at accelerated storage conditions (25 °C). All samples were evaluated in duplicate by parallel test. Two samples were kept for 10 days at 4 °C, and two samples were kept for 4 days at 25 °C. Photographs of the packages were taken at specific time intervals. Colour analysis was performed using the smartphone app and correlated with storage time.

2.8. $CuGluc_2$-PEC colour parameters

The colour changes of $CuGluc_2$-PEC were investigated by employing the CIE 1931 RGB (Red, Green, Blue) colour space (Panunzi, Diana, & Caruso, 2019). CIE calculation was performed by the mobile app named “RGB Colour Detector”. The app can be downloaded for free in the Playstore by Android. The RGB colour intensity was recorded by holding the smartphone camera (Samsung S23) approximately 1 cm from each sample in indirect daily light. The value was obtained by averaging 10 points of the label. The statistical analysis was performed by the ANOVA by SPSS 22.0 (SPSS Statistical Software, Inc., Chicago, IL, USA) package included in Origin 8.5.0 SR1 with the confidence interval set to 95 % to determine the significant difference between specific means.

All colorimetric tests were performed directly after the use. To check the chemical and colorimetric stability of the sensor after extended storage, some sensing labels (one for each type of food) were sealed and stored in dim light under standard humidity conditions at 25 °C for one month. In the same conditions, some used labels (one for each type of food sample) were sealed and stored for two months after use. No colorimetric or morphological changes were observed on these sealed samples.

2.9. Theoretical calculations

Ab initio calculations were performed by Tight Binding (TB) and Density Functional Theory (DFT) using ORCA 6.0.2 software (XTB is integrated in ORCA). GFN2-xTB Hamiltonians (Bannwarth, Ehlert, & Grimme, 2019) were employed (F. Neese, 2012, 2018; Frank Neese, Wennmohs, Becker, & Riplinger, 2020). The TB method was used for the preliminary screening of the solvation process, guessing different structures with an increased fixed number of explicit water molecules. DFT analysis based on the B3LYP functional and a double zeta def2-SVP basis set ensures an accurate and computationally affordable representation of electronic interactions based on simple calculations of optimized geometries as already tested in our previous works(Pascale, D'Arco, Silvio Gentile, & Dovesi, 2022; Platonenko, Gentile, Maul, Pascale, Kotomin, & Dovesi, 2019).The Grimme D3 correction (Stefan Grimme, Antony, Ehrlich, & Krieg, 2010; S. Grimme, Ehrlich, & Goerigk, 2011) was adopted to evaluate the dispersion energies. The implicit solvent method via the ALPB (in TB calculation)(Sigfridsson & Ryde, 1998) and CPCM (in DFT modelling) (Tomasi, Mennucci, & Cammi, 2005) was used to approximate the aqueous environment while accounting for effects on the stability and electronic properties of the complex. The final molecular model of the copper (II) complex with gluconates and water molecules was built by including 20 explicit water molecules supplemented with the implicit CPCM solvent treatment. Energy values were evaluated for models containing 4, 6, 8, 10, 20, and 30 explicit water molecules, obtaining the energy stabilization of the 20 water molecules solvated complex.

3. Results and discussion

3.1. Design and colorimetric response of $CuGluc_2$

The coordination chemistry of copper with donor atoms is complex. The reactivity of copper is reflected in its biological roles in metalloenzymes and proteins, mostly resting in its redox-active character (Modec, Podjed, & Lah, 2020). Under oxidizing conditions, copper exists as Cu (II) (with the related blue or green compounds because of d–d absorptions in the 600 to 900 nm region), while under reducing conditions as Cu (I) (mainly colourless). Typically, Cu (I) compounds are readily oxidized to Cu (II) compounds by oxygen. In a complex system where both amines and thiols are present, copper can be involved in multiple equilibria (Tarkhanova, Gantman, Chizhov, & Smirnov, 2010). Generally, the Cu (II) complexes present in aqueous environments show a facile substitution chemistry with amines, generating different blue complexes depending on the donor ligands (Velásquez-Yévenes & Ram, 2022). On the other hand, Cu-catalysed thiol oxidation is a known process (Kreitman, Danilewicz, Jeffery, & Elias, 2017; Smith et al., 1994). The metal-catalysed oxidation is a described method for the selective oxidation of thiols to disulfides and organic polysulfanes (Kreitman, Danilewicz, Jeffery, & Elias, 2016b) where a change of the oxidation number of the metal cation takes place along with the interaction of the sulfur ligand with the metal. Moreover, the presence of N-based ligands increases the oxidation activity of the metal, and different Cu (II) amino complexes can direct the interaction with various thiols synergistically (Crmarić & Bura-Nakić, 2023).

In our system, the $CuGluc_2$ salt is mixed with pectin in the form of a hydrogel. In this case, the Cu (II) cation is mobile and can react with amino species and thiols generated by food spoilage reactions, producing colored complexes and precipitates. As a plethora of VOCs are produced in the vapor of spoiling food, we can assume an overall colorimetric response due to the reaction of copper (II) with both TVB-Ns and VSCs. A schematic rationalization was attempted by separately reacting $CuGluc_2$ with hydrogen sulfide, ethyl mercaptan, TMA, and ammonia. In an aqueous environment, copper (II) is assumed to be involved in a coordination equilibrium including up to six water molecules (Gómez-Salces, Aguado, Valiente, & Rodriguez, 2012). In the form of an aquo-complex, it involves at least three different reactions, as schematized in Fig. 2. In the same figure, a representation of the different colorimetric responses based on the different possible reactions involving the indicator is proposed. The color of the sensor intensifies over time, from cream to sepia color, due to three responsive processes occurring together. The color depends on the percentage combination of the three reactions, which occur in different proportions and at different times depending on the food sample. Basically, an abundance of H_2S results in a more blackish color, while thiols and amines produce a lighter color, tending towards yellow or bluish respectively. On the other hand, sulfur compounds are particularly insoluble and cause copper to be removed from other possible equilibria. Therefore, a predominance of brown over blue is expected.

The coordination reaction of the copper cation in $CuGluc_2$ with amines was examined by carrying out titration experiments (Fig. 3) on ammonia or TMA solutions in deionized water. Upon reaction of $CuGluc_2$ with H_2S, we recovered the highly insoluble black colloidal CuS precipitate in a virtually quantitative yield, as expected due to the low Kps ($6{\cdot}10^{-37}$, (Myers, 1986)). On the other hand, the oxidation of thiols by copper (II) is a well-described process (Smith et al., 1994), proceeding by formation of a complex between Cu(II) and thiol, oxidation of the thiol to the corresponding radical to form the corresponding disulfide RSSR, and reduction of Cu (II) to Cu(I). In our case, the binding of

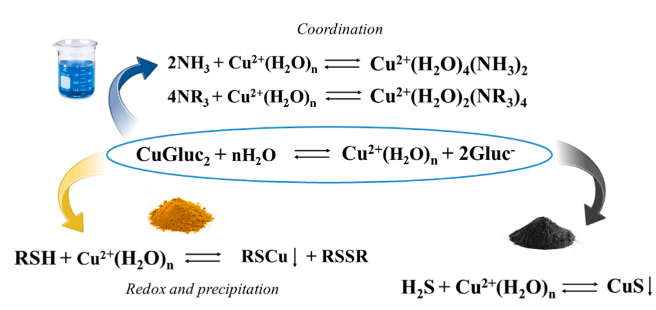

Fig. 2. A summary of the reactions involving $CuGluc_2$ indicator in a humid environment and the related colorimetric response.

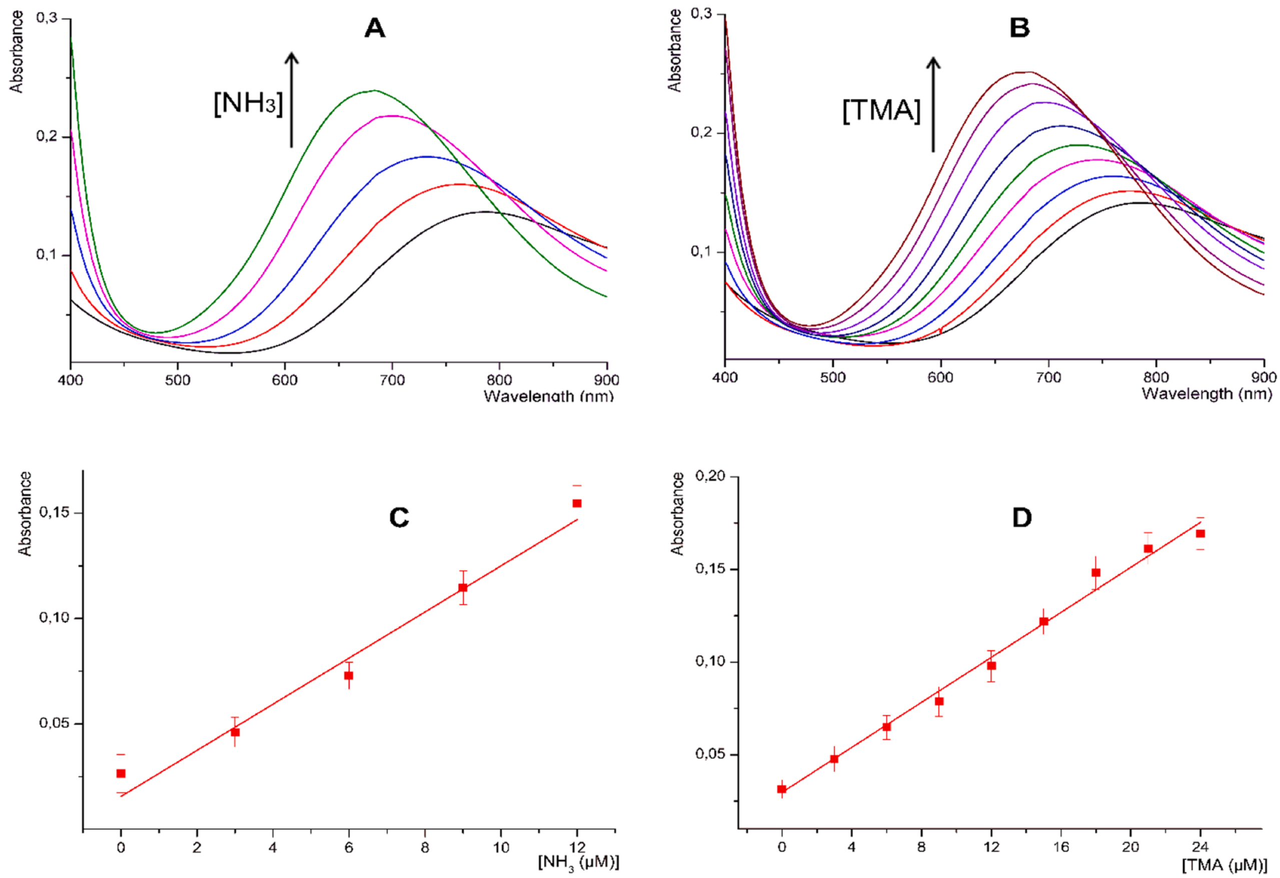

Equation	y = a + b*x		
Residual Sum of	2,36436E-4		
Pearson's r	0,98898		
Adj. R-Square	0,97077		
		Value	Standard Error
	Intercept	0,01797	0,00688
	Slope	0,01083	9,35783E-4

Equation	y = a + b*x		
Residual Sum of Squares	1,97049E-4		
Pearson's r	0,99517		
Adj. R-Square	0,98899		
		Value	Standard Error
	Intercept	0,02887	0,00326
	Slope	0,00613	2,28319E-4

Fig. 3. Titration experiment obtained by recording UV–vis absorption spectra of $CuGluc_2$ as a function of NH_3 (A) and TMA (B) concentration (analyte concentration increasing according to the arrow). Plot of the absorbance maximum as a function of concentration for TMA (C) and NH_3 (D). The wavelength peak used for regression data is 675 nm.

ethyl thiol to Cu (II) resulted in the reduction of the Cu (II) cation to the Cu (I) cation, present in the copper-thiolate (CuSEt) species (Kreitman, Danilewicz, Jeffery, & Elias, 2016a) which aggregates in a yellow precipitate, further stabilizing the Cu (I) ion. Yield is virtually quantitative, also in this case (Rosita Diana, Caruso, Piotto, Concilio, Shikler, & Panunzi, 2020; Mandal, Das, Singh, Shukla, & Bharadwaj, 1997).

The Cu (II) cation is known to be able to coordinate nitrogen-based ligands in aqueous environments. Humidity plays a critical role in the sensor performance (Silva et al., 2024). As we did not conduct experiments in dry storage (we sealed the food samples in standard humidity conditions) the humidity is assumed to be significant in the presence of food, both in refrigerated conditions and at room temperature (Protopappas, Bechtsis, & Tsotsolas, 2025). The copper (II) cation in a humid environment is supposed to be in an octahedral coordination. (Nguyen, Gulaczyk, Kręglewski, & Kleiner, 2021; Pecsok & Juvet, 1955; van Haveren, van Bekkum, & Peters, 1993). As discussed below, the coordination is assumed to involve two *O,O* chelating gluconate ions in a square planar arrangement and two apical water molecules (Cai et al., 2023; Di, Zhang, Liu, Kong, & Zhou, 2021) though different nucleophilicity and coordinating abilities can give adducts of different stoichiometry. In the titration of $CuGluc_2$ with ammonia, by increasing ammonia concentration, the absorption band of $CuGluc_2$ originally recorded at 781 nm (black curve in Fig. 3, panel A) increases and blue shifts, reaching a maximum at two equivalents of NH_3 (at 665 nm, Fig. 3, panel A). This can be ascribed to the replacement of two water molecules in the copper coordination sphere. The strong nucleophile character of TMA is reflected in the adduct 1:4 Cu/TMA (Henderson Jr & Schultz, 1962). By increasing TMA concentration, the maximum absorption band of $CuGluc_2$ at 781 nm increases and blue shifts, reaching a maximum at four equivalents of TMA (at 670 nm, Fig. 3, panel B). In such conditions, we can assume that four TMA molecules replace two water molecules and two coordinated hydroxyl groups around the copper cation (Fig. 4). In both titration experiments, the absorption signal for subsequent additions increases and slightly red shifts. This must be related to the increase in pH and not to obvious changes in the coordination sphere.

The LOD values (90 μM for NH_3 and 55 μM for TMA) were found based on $3\sigma/k$ value, where σ is the standard deviation of blank measurement, and k is the slope of the plot of absorption versus analyte concentration. Accordingly, the LOQ values were found 300 μM for NH_3 and 183 μM for TMA. The sensitivity was found 0.97 μM for NH_3 and 0.34 μM for TMA ($\sigma = 6.88$ and 3.26, respectively).

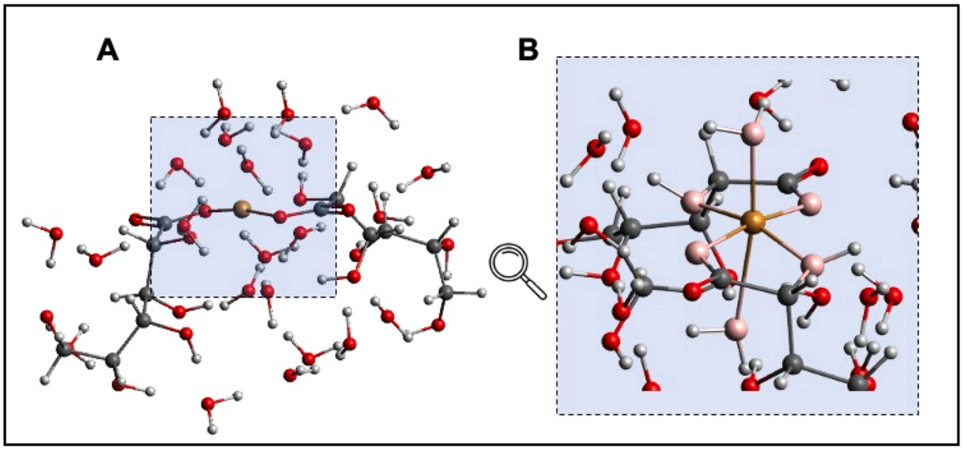

Fig. 4. The optimized B3LYP geometry of $CuGluc_2 \cdot 2H_2O$ (panel A). Enlarged detail of the coordination site (panel B) where the blue dashed lines represent the ligand-metal distance, indicated in Å.

3.2. Theoretical approach to $CuGluc_2$ in an aqueous environment

A representative model of $CuGluc_2$ in an aqueous environment was derived by the theoretical approach starting from the assumption of the typical octahedral geometry of solvated copper (II) complexes. As in other gluconate salts (Cai et al., 2023) two *O,O* chelating gluconate ligands were placed in the equatorial plane of the copper complex. The gluconate groups chelate the metal cation by the mono-negative oxygen atom of the carboxylate group and the oxygen atom of the OH group on the β carbon. Two thermodynamically favored five-membered rings form in the equatorial plane of the complex. Two water molecules are assumed to complete the coordination sphere at the axial positions. Starting from this structural pattern, a combination of computational approaches was employed to evaluate the conformations of the complex $CuGluc_2 \cdot 2H_2O$. The global minimum search was achieved by gradient minimization along the potential energy surface (PES). Due to the significant H-bond interactions of the carbohydrate moieties in an aqueous environment, the use of an implicit solvent via the CPCM model did not provide an accurate description of the interaction between $CuGluc_2$ and the aqueous medium. The optimization was performed by using the ORCA SOLVATATION tool, which produced a hydration sphere of 20 water molecules on the model $CuGluc_2 \cdot 2H_2O$.

The combination of hydrogen bonds and coordination interactions determines the overall conformation of the complex. The optimized geometry confirmed hexa-coordination in a distorted octahedral geometry with six binding oxygen atom groups (Fig. 4). As expected, the strongest interaction is due to the negative oxygen of the carboxylate group (O5 and O27 oxygens) with shorter Cu–O bond distances (1.948 Å and 1.953 Å) and quite high Mayer bond orders (0.501 and 0.470, respectively). The β hydroxyl groups (O3 and O25 oxygens) show shorter Cu-O distances (1.980-2.189 Å) and lower Mayer bond orders (0.391 and 0.408). Two water molecules (O46 and O48 oxygens) are placed at 2.189 Å and 2.709 Å, with slightly negative Mayer bond orders (-0.3235 and -0.365). The two water molecules and two β hydroxyl groups are the weak ligands completing the coordination sphere. However, the bond distance and the Mayer bond order values assign them a specific coordination role rather than a simple electrostatic interaction. Based on these considerations, the replacement of two water molecules by ammonia and of the four weak ligands by TMA (see Sect. 3.1) can be confirmed.

3.3. Application of $CuGluc_2$-PEC for monitoring chicken, salmon, and shrimp' spoilage

For each $CuGluc_2$-PEC label, about 100 mg of $CuGluc_2$, 400 mg of pectin, and 600 mg of PVA were used. For the experiments we used pectin and PVA by Sigma-Aldrich (≈ 99 % purity) while the copper salt was a pharmacy product used for dietary supply (99+ % purity). However, the focus on sustainability required assessing the feasibility and cost of the indicator when using food-grade ingredients commonly found in large-scale retail outlets. Low-cost food-grade PVA and pectin easily sourced were also used (see Materials and Methods). Tests carried out using common pectin and PVA give the same colorimetric result, confirming the purely carrier action of pectin and the purely adhesive action of PVA. Using widely available products, the cost of the packages for a private buyer was: 1Kg of PVA 21.9 euro; 1Kg of pectin 86 euro; 100 g of copper (II) gluconate 13 euro. In this case, the unit cost per label is estimated at 5–6-euro cents, compared to 40–50-euro cents for the certified chemicals. Obviously, industrial-scale production would still lead to cost reductions.

The $CuGluc_2$-PEC indicator proved to be a multipurpose freshness indicator by capturing volatile amines and thiols of high-perishability and short-shelf-life protein foods. The indicator was applied to monitor chicken, salmon, and shrimp spoilage marketed in packs. Their chemical compositional changes during storage result in the production of TVB-Ns and VSCs as biomarkers of protein degradation. The gradually produced TVB-Ns mainly consist of NH_3 and volatile amines, while VSCs include H_2S and mercaptans (Kuuliala et al., 2018; Mikš-Krajnik, Yoon, Ukuku, & Yuk, 2016; Mikš-Krajnik, Yoon, & Yuk, 2015). The colour change of the sensor is assumed associated with the increase in such kind of VOCs thanks to three different reactions of $CuGluc_2$ with the analytes (see Sect.3.1).

The colour monitoring was carried out for all food samples from day 0 (packaging day) up to day 4 at 25 °C (Fig. 5), and from day 0 to day 14 at 4 °C (Fig. 6). In both experiments, $CuGluc_2$-PEC was placed in the PS tray containing commercial food samples and wrapped in cling film under sterile conditions. The chromatic variation of the $CuGluc_2$-PEC indicator over time is a reliable visual indicator of spoilage. Generally, the initial color of the indicator (day 0) is perceived as light beige, which gradually intensifies over time to dark brown or blackish. The main colorimetric components are yellow, black, and blue. Storage temperature, which is a limitation of many sensing tools, is not a critical issue. The $CuGluc_2$-PEC indicator results are effective within and beyond the expiry date of the products, both in accelerated spoiling conditions (25 °C) and at refrigerated temperature (4 °C).

In the experiments carried out at 25 °C, the colour of the indicator rapidly intensifies starting from the first 24 h. On day 4, when the product is clearly “spoiled,” the colour is blackish brown. The corresponding R/B colour parameters as a function of time increase accordingly (diagram in Fig. 5). As expected, (I. N. A. Ashie, Smith, Simpson, & Haard, 1996; Kuuliala et al., 2018; Mikš-Krajnik et al., 2016; Mikš-Krajnik et al., 2015) the colorimetric response is sharper with shrimp,

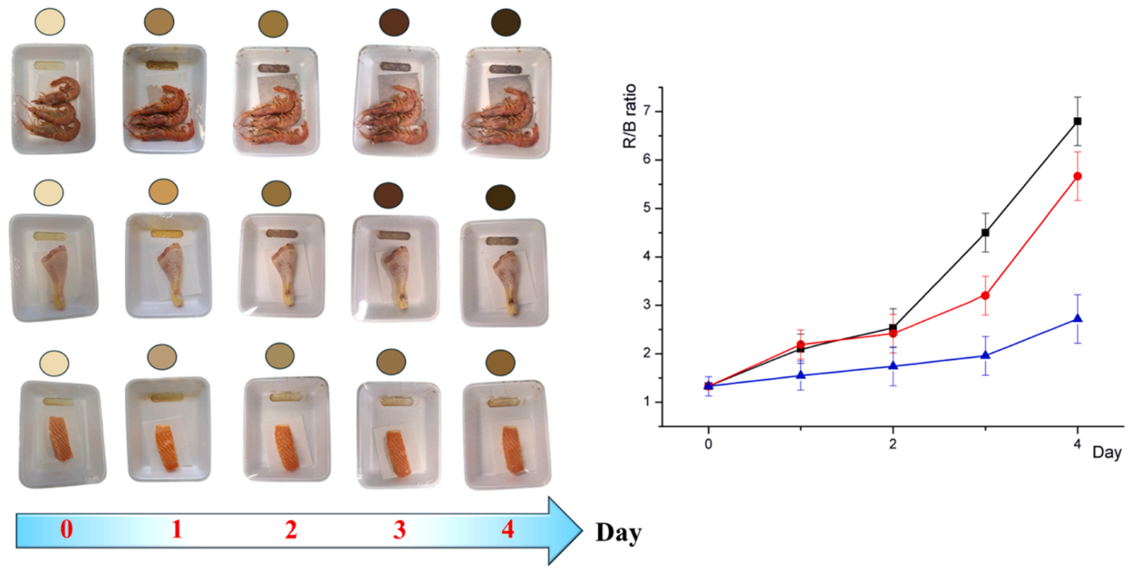

Fig. 5. Visual monitoring of packaged chicken, salmon, and shrimp's freshness at 25 °C for 4 days (photograph in natural diffused and shadowed light). Corresponding R/B colour parameters as a function of time (black curve for shrimp, red curve for chicken, blue curve for salmon).

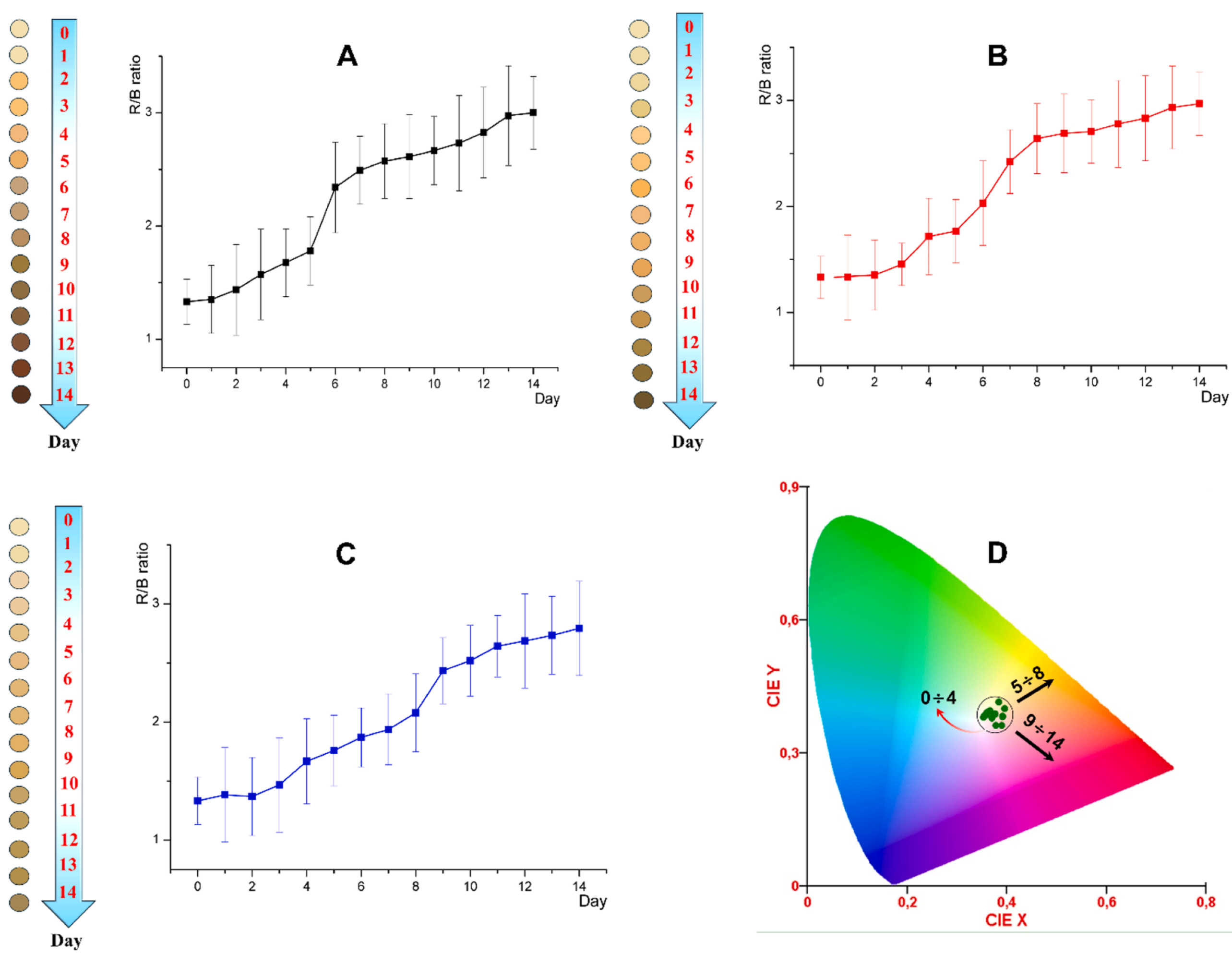

Fig. 6. Label color (on the left) for visual monitoring of freshness of shrimp (panel A), chicken (panel B), and salmon (panel C) packaged at 4 °C for 14 days (photographed in diffused natural light and shade). Corresponding R/B colour parameters (panel D) as a function of time for days 0-4 (in the red ring). The black arrows indicate the shift in the CIE colorimetric parameters on days 5-8 and 9-14, respectively.

more evident than with chicken and salmon meat.

In the experiments carried out at 4 °C (correct storage conditions) for

14 days (Fig. 6), the colour of the indicator does not vary continuously and undergoes the first relevant change starting from days 4-5. Concerning the expiry date (indicated on the same marketed foods stored at 4 °C), the sample can be considered fresh for 4 days following packaging (Das & Mishra, 2023; Mikš-Krajnik et al., 2016; Zouharová et al., 2023). The colour and the R/B parameters remain quite constant for days 0-4, cluster for all food samples in the small area delimited by a circle in the CIE diagram of Fig. 6D (both x and y values vary between 0.35 and 0.40). Starting from day 5, the colour intensifies accordingly with the corresponding black arrow. From day 8 to day 10, when the samples are expected to proceed from spoiling to spoiled (Zouharová et al., 2023) the colour turns to blackish brown moving along the corresponding black arrow in the CIE diagram. The color of the label is indicative of the gaseous phase rich in TVB-Ns and VSCs products. The pattern is evident for shrimp and chicken samples (as in the test at 25 °C). A more gradual pattern is recorded for the salmon samples.

3.4. SEM and GC analysis

The morphology of each single layer and the whole $CuGluc_2$-PEC label before and after use as an intelligent packaging (used sensor) was investigated by SEM analysis. In Table 1 are summarised the weight concentration of the elements on the surface of the layers. The neat polymer layers (PS, PVA, pectin) were checked for method confirmation. In that case, mainly carbon atoms for PS, and carbon and oxygen atoms for PVA and pectin were detected.

SEM micrographs of the surface of the multilayer label $CuGluc_2$-PEC acquired at 3800x and 8800x (Fig. 7) show a surface with an irregular distribution of micropores, rounded and of variable dimensions. The porous structure can be attributed to the drying process of the cupric salt on the pectin layer, while some micro-inhomogeneity can be due to the swelling of the pectin when the cupric solution is added. Interestingly, no significant undissolved crystals remain after the absorption of $CuGluc_2$ on the substrate. The amorphous and holed habitus offer an advantage as a permeable medium, where equilibria occur easily and rapidly in a humid environment.

Although EDS results can be influenced by various factors, such as surface roughness and matrix effects, the average results were consistent and interesting. This is especially true because this technique allowed us to obtain results related to the surface layer. For the elemental analysis, SEM-EDS technique was employed by analysing 10 different points for each sample and the results were reported in Table 1 (for the neat polymeric layers and the unused $CuGluc_2$-PEC label) and in Table 2 (for the used $CuGluc_2$-PEC labels) as an average. The elemental analysis performed on the unused $CuGluc_2$ deposited onto the pectin layer ($CuGluc_2$-PEC label) shows the presence of sodium ions (a ubiquitous pollutant). SEM analysis of the indicator surface was collected at the end of the spoilage process of all food samples at 25 °C and 4 °C (Table 2). Although VSCs and TVB-Ns produced during spoilage depend on time, thermal history, microbial contamination, food origin, and quality (Bekhit, Holman, Giteru, & Hopkins, 2021), SEM analysis of the used sensors highlights some trends. The colorimetric response can be cross-checked with the SEM data. First, based on sulfur and nitrogen content, the decomposition degree after 5 days at 25 °C is greater than after 2 weeks at 4 °C. The colour parameters generally align with SEM data (R/B final values in Fig. 5 are larger than those in Fig. 6). The ratio between nitrogen and sulfur (N/S) content at 25 °C is comparable to the N/S ratio at 4 °C for each kind of food sample. The salmon samples have low sulfur content compared to the chicken and shrimp samples. Since the precipitates of copper (II) sulfide turn to a darker color, we can explain the lighter color of the label used for the salmon samples. The diagram in Fig. 6 relating to spoilage in accelerated conditions is explanatory, where the R/B values are respectively: 4.50 and 6.81 for shrimp, 3.23 and 5.68 for chicken, and 1.96 and 2.71 for salmon samples. However, additional information was obtained from GC analysis of VOCs produced by each food. Samples of salmon, chicken, and shrimp were sealed in airtight containers equipped with a septum for perforation. A micro syringe was used to collect the VOCs. The headspace gas produced by the food samples in the accelerated spoilage conditions (after 5 days at 25 °C) was introduced into the GC column. The volatile molecules collected at the end of the spoilage process of all food samples at 25 °C were reported in Table 3 (an offprint of the complete VOCs analysis certificate, reported in the Supplementary Materials).

Confirming the SEM results on the used labels, TVB-Ns are higher in the spoiled salmon samples than in the chicken and shrimp samples (see TMA in Table 3). Ammonia significantly contributes to the nitrogen content of all food products. As for the label's response, this should lead to a blue-green color. As for VSCs, hydrogen sulfide, which produces black precipitate with Cu (II) ion, is maximum for the shrimp, much lower for the chicken, and very low for the salmon. An additional contribution to the sulfur atom comes from methyl mercaptan, which binds to the sensor, producing a yellow ochre color. Sulfides do not produce a reaction with the label. The GC analysis aligns with SEM data, revealing an abundance of sulfur in the chicken' VOCs, less in the shrimp' VOCs, and low in the salmon' VOCs. As for the colorimetric response, the blackish color of the shrimps' label, less intense than the chicken's label, and even more of the salmon's label, is not purely related to the quantity of sulfur but rather to the type of sulfur compound. Hydrogen sulfide appears maximally from the third day onwards, as it is generated in a less aerobic environment when the product is significantly spoiling (Tian, Xi, Yeung, & Ren, 2020). Therefore, the change to a dark tone color in the label (days 9-14 in the CIE colorimetric diagram of Fig. 6) can be considered a temporal indicator of actual food spoilage.

Table 1
SEM-EDS weight concentration data of main atoms on the surface of the neat polymeric layers and the unused $CuGluc_2$-PEC label. Data mediated on 10 points.

Layer (formula)	Calc. element conc. (% w/w)	Exp. element conc. (% w/w)
PS $(C_8H_8)_x$	C: 92.3	C: 93.4
PVA $(C_2H_4O)_x$	C:54.5; O:36.3	C:56.4; O:34.8
Pectin $(C_7H_{20}O_6)_x$	C:41.9; O:47.9	C:43.1; O:51.8
$CuGluc_2$-PEC ($C_{12}H_{22}CuO_{14}$)	C:36.8; O:45.3; Cu:10.0	C:31.8; O:49.3; Cu:14.0

4. Conclusions

In today's market, sustainability is the watchword. It is a key factor influencing consumer and producer decisions. Eco-labels have become an essential component of sustainable packaging. Following the demand for sustainability, we have designed a smart label for monitoring protein foods. A polymeric multilayer film was produced, based on the food-grade $CuGluc_2$ salt immobilized on a pectin matrix and grafted by PVA to a commercial PS packaging. The obtained label, made with eco-friendly ingredients, acts as a soft matter sensor. The responsive mechanism involves coordination, redox, and precipitation reactions between the cupric ion and some N- and S-containing VOCs. In the tests performed on fresh chicken, salmon, and shrimp, a gradual chromatic variation of the label over time resulted a reliable visual indicator of spoilage at 25 °C and at 4 °C. The initial color of the indicator perceived as light beige intensifies over time to dark brown or blackish, due to the combination of three colors (yellow, blue, black) depending on three different reactions. With a Samsung S23 smartphone camera we were able to record the evolution of the RGB pattern day by day, demonstrating the sensor's ability to indicate food freshness effectively. Also, we attempted to establish a correlation between the population of VOCs and the colorimetric response by crossing SEM-ESD and GC analysis. In conclusion, we can claim the affordability and sustainability of the smart label, in addition, the response speed, durability, and effectiveness at low temperatures. Further analysis is needed for a commercial-scale

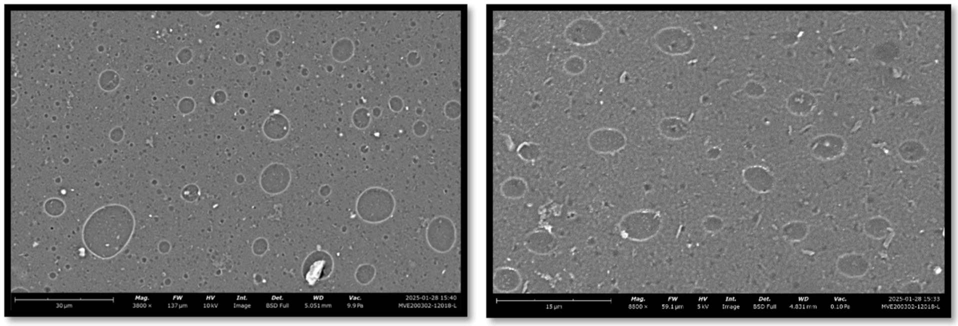

Fig. 7. SEM micrographs of the $CuGluc_2$-PEC surfaces at magnifications and scale bars: 3800x (on the left) and 8800x (on the right).

Table 2
SEM-EDS weight concentration data of nitrogen and sulfur atoms on the surface of the used $CuGluc_2$-PEC label after 5 days at 25 °C and after 14 days at 4 °C. Samples were evaluated in duplicate by parallel test. Data mediated on 10 points.

Food sample	Nitrogen (% w/w) 25 °C 4 °C	Sulfur (% w/w) 25 °C 4 °C
Salmon	12.1 ± 0.4 10.7 ± 0.3	0.97 ± 0.05 0.71 ± 0.04
Shrimp	7.7 ± 0.3 6.6 ± 0.2	4.1 ± 0.2 3.6 ± 0.2
Chicken	1.74 ± 0.07 1.02 ± 0.04	30.3 ± 0.9 20.4 ± 0.6

Table 3
Concentration (mg/m^3) of the most abundant TVB-Ns and VSCs after 5 days at 25 °C by headspace GC analysis. *) Ammonia concentration (mg/m^3) by titration (UNI ISO 2365:2023 method, measurement uncertainty 12.1 %). Original certificate of analysis produced according to the laboratory's EPA TO 15A 2019 method reported in the Supplementary Materials.

TVB-Ns	**salmon**	**shrimp**	**chicken**
TMA	8.0	6.7	0.75
Acetonitrile	0.001	0.003	0.002
NH_3*)	144	270	240
VSCs	**salmon**	**shrimp**	**chicken**
H_2S	0.025	57.1	2.45
$(CH_3)_2S$	1.05	0.18	0.62
$(CH_3)_2S_2$	21	7.0	18.2
isopropyl mercaptan	<0.001	<0.001	0.021
metyl mercaptan	8.9	2.1	260

perspective. However, this study lays the foundation for the development of non-invasive low-cost sensory labels for existing commercial packaging.

Funding

This research was funded by the project "CASES - Cartoni ondulati idonei per il contatto con Alimenti, rivestiti Superficialmente con coating Ecocompatibili, biodegradabili e compostabili a base di pectine e Sieroproteine"– CUP C77B23000070005.

Declaration of ethical statement - studies in humans and animals

The authors declare that studies in humans and animals are not involved.

CRediT authorship contribution statement

Ludovica Milzi: Methodology, Conceptualization. **Rosita Diana:** Writing – review & editing, Writing – original draft, Visualization, Validation, Supervision, Methodology, Investigation, Data curation, Conceptualization. **Francesco Silvio Gentile:** Formal analysis, Data curation. **Pasquale Ferranti:** Writing – review & editing, Data curation. **Ugo Caruso:** Data curation. **Fabio Mazzaglia:** Methodology, Data curation. **Barbara Panunzi:** Writing – review & editing, Writing – original draft, Supervision, Resources, Project administration, Investigation, Funding acquisition.

Declaration of competing interest

The authors declare the following financial interests/personal relationships which may be considered as potential competing interests: Barbara Panunzi reports financial support was provided by Ministry of Education University and Research.

Supplementary materials

Supplementary material associated with this article can be found, in the online version, at doi:10.1016/j.afres.2026.101717.

Data availability

No data was used for the research described in the article.

References

Abedi-Firoozjah, R., Bahramian, B., Tavassoli, M., Ahmadi, N., Noori, S. M. A., Hashemi, M., … Jafari, S. M. (2025). A comprehensive review of gum-based electrospun nanofibers for food packaging: Preparation, developments, and potential applications. *International Journal of Biological Macromolecules, 288*, Article 138717. https://doi.org/10.1016/j.ijbiomac.2024.138717

Abedi-Firoozjah, R., Bahramian, B., Tavassoli, M., Majlesi, M., Ghaderi, S., Assadpour, E., … Jafari, S. M. (2025). Alginate-based edible films/coatings/nanofibers in food packaging: A comprehensive review of recent advances. *Carbohydrate Polymer Technologies and Applications, 11*. https://doi.org/10.1016/j.carpta.2025.100955

Abedi-Firoozjah, R., Chabook, N., Rostami, O., Heydari, M., Kolahdouz-Nasiri, A., Javanmardi, F., … Mousavi Khaneghah, A. (2023). PVA/starch films: An updated review of their preparation, characterization, and diverse applications in the food industry. *Polymer Testing, 118*. https://doi.org/10.1016/j.polymertesting.2022.107903

Ashie, I. N., Smith, J. P., & Simpson, B. K. (1996). Spoilage and shelf-life extension of fresh fish and shellfish. *Critical Reviews in Food Science and Nutrition, 36*(1-2), 87–121. https://doi.org/10.1080/10408399609527720

Ashie, I. N. A., Smith, J. P., Simpson, B. K., & Haard, N. F. (1996). Spoilage and shelf-life extension of fresh fish and shellfish. *Critical Reviews in Food Science and Nutrition, 36* (1-2), 87–121. https://doi.org/10.1080/10408399609527720

Balbinot-Alfaro, E., Craveiro, D. V., Lima, K. O., Costa, H. L. G., Lopes, D. R., & Prentice, C. (2019). Intelligent Packaging with pH Indicator Potential. *Food Engineering Reviews, 11*(4), 235–244. https://doi.org/10.1007/s12393-019-09198-9

Bannwarth, C., Ehlert, S., & Grimme, S. (2019). GFN2-xTB—An accurate and broadly parametrized self-consistent tight-binding quantum chemical method with multipole electrostatics and density-dependent dispersion contributions. *Journal of Chemical Theory and Computation, 15*(3), 1652–1671. https://doi.org/10.1021/acs.jctc.8b01176

Bekhit, A. E.-D. A., Holman, B. W. B., Giteru, S. G., & Hopkins, D. L. (2021). Total volatile basic nitrogen (TVB-N) and its role in meat spoilage: A review. *Trends in Food Science & Technology, 109*, 280–302. https://doi.org/10.1016/j.tifs.2021.01.006

Bhargava, N., Sharanagat, V. S., Mor, R. S., & Kumar, K. (2020). Active and intelligent biodegradable packaging films using food and food waste-derived bioactive compounds: A review. *Trends in Food Science & Technology, 105*, 385–401. https://doi.org/10.1016/j.tifs.2020.09.015

Cai, D.-H., Liang, B.-F., Chen, B.-H., Liu, Q.-Y., Pan, Z.-Y., Le, X.-Y., & He, L. (2023). A novel water-soluble Cu(II) gluconate complex inhibits cancer cell growth by triggering apoptosis and ferroptosis related mechanisms. *Journal of Inorganic Biochemistry, 246*, Article 112299. https://doi.org/10.1016/j.jinorgbio.2023.112299

Chiellini, E., Corti, A., D'Antone, S., & Solaro, R. (2003). Biodegradation of poly (vinyl alcohol) based materials. *Progress in Polymer Science, 28*(6), 963–1014. https://doi.org/10.1016/S0079-6700(02)00149-1

Crmarić, D., & Bura-Nakić, E. (2023). Interaction between Cu and thiols of biological and environmental importance: Case study using combined spectrophotometric/bathocuproine sulfonate disodium salt hydrate (BCS) assay. *Molecules, 28* (Vol.).

Das, J., & Mishra, H. N. (2023). A comprehensive review of the spoilage of shrimp and advances in various indicators/sensors for shrimp spoilage monitoring. *Food Research International, 173*, Article 113270. https://doi.org/10.1016/j.foodres.2023.113270

Delgado-Rodríguez, M., Ruiz-Montoya, M., Giraldez, I., López, R., Madejón, E., & Díaz, M. J. (2012). Use of electronic nose and GC-MS in detection and monitoring some VOC. *Atmospheric Environment, 51*, 278–285. https://doi.org/10.1016/j.atmosenv.2012.01.006

Di, Y.-Y., Zhang, G.-C., Liu, Y.-P., Kong, Y.-X., & Zhou, C.-S. (2021). Crystal structure and thermodynamic properties of the coordination compound calcium D-gluconate Ca [D-C6H11O7]2(s). *Journal of Molecular Structure, 1225*, Article 128818. https://doi.org/10.1016/j.molstruc.2020.128818

Diana, R., Caruso, U., Di Costanzo, L., Bakayoko, G., & Panunzi, B. (2020). A novel DR/NIR T-shaped aiegen: Synthesis and x-ray crystal structure study. *Crystals, 10*(4). https://doi.org/10.3390/cryst10040269

Diana, R., Caruso, U., Di Costanzo, L., Gentile, F. S., & Panunzi, B. (2021). Colorimetric recognition of multiple first-row transition metals: A single water-soluble chemosensor in acidic and basic conditions. *Dyes and Pigments, 184*. https://doi.org/10.1016/j.dyepig.2020.108832

Diana, R., Caruso, U., Piotto, S., Concilio, S., Shikler, R., & Panunzi, B. (2020). Spectroscopic behaviour of two novel azobenzene fluorescent dyes and their polymeric blends. *Molecules, 25* (Vol.).

Diana, R., Milzi, L., Gentile, F. S., Pannico, M., Musto, P., Maiello, A., & Panunzi, B. (2024). A versatile pH-sensitive hydrogel based on a high-performance dye: Monitoring the freshness of milk and chicken meat. *Journal of Food Composition and Analysis*, 135. https://doi.org/10.1016/j.jfca.2024.106667

Dordevic, D., Capikova, J., Dordevic, S., Tremlová, B., Gajdács, M., & Kushkevych, I. (2023). Sulfur content in foods and beverages and its role in human and animal metabolism: A scoping review of recent studies. *Heliyon, 9*(4), Article e15452. https://doi.org/10.1016/j.heliyon.2023.e15452

Fan, M., Rakotondrabe, T. F., Chen, G., & Guo, M. (2023). Advances in microbial analysis: Based on volatile organic compounds of microorganisms in food. *Food Chemistry, 418*, Article 135950. https://doi.org/10.1016/j.foodchem.2023.135950

Feng, Y., Wang, Y., Beykal, B., Qiao, M., Xiao, Z., & Luo, Y. (2024). A mechanistic review on machine learning-supported detection and analysis of volatile organic compounds for food quality and safety. *Trends in Food Science & Technology, 143*, Article 104297. https://doi.org/10.1016/j.tifs.2023.104297

Gómez-Salces, S., Aguado, F., Valiente, R., & Rodriguez, F. (2012). Unraveling the coordination geometry of copper(II) ions in aqueous solution through absorption intensity. *Angewandte Chemie - International Edition, 51*(37), 9335–9338. https://doi.org/10.1002/anie.201202033

Grimme, S., Antony, J., Ehrlich, S., & Krieg, H. (2010). A consistent and accurate ab initio parametrization of density functional dispersion correction (DFT-D) for the 94 elements H-Pu. *The Journal of Chemical Physics*, (15), 132. https://doi.org/10.1063/1.3382344

Grimme, S., Ehrlich, S., & Goerigk, L. (2011). Effect of the damping function in dispersion corrected density functional theory. *Journal of Computational Chemistry, 32*(7), 1456–1465. https://doi.org/10.1002/jcc.21759

Han, Y., Xie, N., & Zhou, W. (2024). Copper coordination-based nanomedicine for tumor theranostics. *Advanced Therapeutics, 7*(2), Article 2300305. https://doi.org/10.1002/adtp.202300305

Henderson, W. A., Jr, & Schultz, C. J (1962). The nucleophilicity of amines. *The Journal of Organic Chemistry, 27*(12), 4643–4646.

Jiang, J., Zhang, W., Yi, X., Lei, Q., Liao, Y., Tan, Y., & Yu, W. (2024). Recent progress in properties and application of antibacterial food packaging materials based on polyvinyl alcohol. 24(1). 10.1515/epoly-2023-0097.

Kalpana, S., Priyadarshini, S. R., Maria Leena, M., Moses, J. A., & Anandharamakrishnan, C. (2019). Intelligent packaging: Trends and applications in food systems. *Trends in Food Science & Technology, 93*, 145–157. https://doi.org/10.1016/j.tifs.2019.09.008

Kreitman, G. Y., Danilewicz, J. C., Jeffery, D. W., & Elias, R. J. (2016a). Reaction mechanisms of metals with hydrogen sulfide and thiols in model wine. Part 1: Copper-catalyzed oxidation. *Journal of Agricultural and Food Chemistry, 64*(20), 4095–4104. https://doi.org/10.1021/acs.jafc.6b00641

Kreitman, G. Y., Danilewicz, J. C., Jeffery, D. W., & Elias, R. J. (2016b). Reaction mechanisms of metals with hydrogen sulfide and thiols in model wine. Part 2: Iron- and copper-catalyzed oxidation. *Journal of Agricultural and Food Chemistry, 64*(20), 4105–4113. https://doi.org/10.1021/acs.jafc.6b00642

Kreitman, G. Y., Danilewicz, J. C., Jeffery, D. W., & Elias, R. J. (2017). Copper(II)-mediated hydrogen sulfide and thiol oxidation to disulfides and organic polysulfanes and their reductive cleavage in wine: Mechanistic elucidation and potential applications. *Journal of Agricultural and Food Chemistry, 65*(12), 2564–2571. https://doi.org/10.1021/acs.jafc.6b05418

Kuuliala, L., Abatih, E., Ioannidis, A. G., Vanderroost, M., De Meulenaer, B., Ragaert, P., & Devlieghere, F. (2018). Multivariate statistical analysis for the identification of potential seafood spoilage indicators. *Food Control, 84*, 49–60. https://doi.org/10.1016/j.foodcont.2017.07.018

Lee, K., Park, H., Baek, S., Han, S., Kim, D., Chung, S., … Seo, J. (2019). Colorimetric array freshness indicator and digital color processing for monitoring the freshness of packaged chicken breast. *Food Packaging and Shelf Life, 22*, Article 100408. https://doi.org/10.1016/j.fpsl.2019.100408

Li, A. J., Pal, V. K., & Kannan, K. (2021). A review of environmental occurrence, toxicity, biotransformation and biomonitoring of volatile organic compounds. *Environmental Chemistry and Ecotoxicology, 3*, 91–116. https://doi.org/10.1016/j.enceco.2021.01.001

Lydekaityte, J., & Tambo, T. (2020). Smart packaging: Definitions, models and packaging as an intermediator between digital and physical product management. *The International Review of Retail, Distribution and Consumer Research, 30*(4), 377–410.

Ma, Q., Lu, X., Wang, W., Hubbe, M. A., Liu, Y., Mu, J., … Rojas, O. J. (2021). Recent developments in colorimetric and optical indicators stimulated by volatile base nitrogen to monitor seafood freshness. *Food Packaging and Shelf Life*, 28. https://doi.org/10.1016/j.fpsl.2021.100634

Mandal, S., Das, G., Singh, R., Shukla, R., & Bharadwaj, P. K. (1997). Synthesis and studies of Cu(II)-thiolato complexes: bioinorganic perspectives. *Coordination Chemistry Reviews, 160*, 191–235. https://doi.org/10.1016/S0010-8545(96)01342-2

Mikš-Krajnik, M., Yoon, Y.-J., Ukuku, D. O., & Yuk, H.-G. (2016). Volatile chemical spoilage indexes of raw Atlantic salmon (Salmo salar) stored under aerobic condition in relation to microbiological and sensory shelf lives. *Food Microbiology, 53*, 182–191. https://doi.org/10.1016/j.fm.2015.10.001

Mikš-Krajnik, M., Yoon, Y.-J., & Yuk, H.-G. (2015). Detection of volatile organic compounds as markers of chicken breast spoilage using HS-SPME-GC/MS-FASST. *Food Science and Biotechnology, 24*(1), 361–372. https://doi.org/10.1007/s10068-015-0048-5

Milzi, L., Diana, R., & Panunzi, B. (2025). Visual food sensing: The state-of-the-art through strategies, tools, analytes, and actual applications. *Journal of Food Composition and Analysis*, 139. https://doi.org/10.1016/j.jfca.2024.107096

Modec, B., Podjed, N., & Lah, N. (2020). Beyond the Simple Copper(II) coordination chemistry with quinaldinate and secondary amines. *Molecules, 25* (Vol.).

Myers, R. J. (1986). The new low value for the second dissociation constant for H2S: Its history, its best value, and its impact on the teaching of sulfide equilibria. *Journal of Chemical Education, 63*(8), 687. https://doi.org/10.1021/ed063p687

Neese, F. (2012). The ORCA program system. *Wiley Interdisciplinary Reviews: Computational Molecular Science, 2*(1), 73–78. https://doi.org/10.1002/wcms.81

Neese, F. (2018). Software update: the ORCA program system. version 4.0. *Wiley Interdisciplinary Reviews: Computational Molecular Science, 8*(1). https://doi.org/10.1002/wcms.1327

Neese, F., Wennmohs, F., Becker, U., & Riplinger, C. (2020). The ORCA quantum chemistry program package. *The Journal of Chemical Physics*, (22), 152. https://doi.org/10.1063/5.0004608

Nguyen, H. V. L., Gulaczyk, I., Kręglewski, M., & Kleiner, I. (2021). Large amplitude inversion tunneling motion in ammonia, methylamine, hydrazine, and secondary amines: From structure determination to coordination chemistry. *Coordination Chemistry Reviews, 436*, Article 213797. https://doi.org/10.1016/j.ccr.2021.213797

Nikolaou, V., Anastasaki, A., Alsubaie, F., Simula, A., Fox, D. J., & Haddleton, D. M. (2015). Copper(ii) gluconate (a non-toxic food supplement/dietary aid) as a precursor catalyst for effective photo-induced living radical polymerisation of acrylates11Electronic supplementary information (ESI) available: Synthesis details, NMR spectra, SEC chromatograms, MALDI spectra and crystallographic details. See 10.1039/c5py00406c *Polymer Chemistry, 6*(19), 3581–3585. https://doi.org/10.1039/c5py00406c.

Panunzi, B., Diana, R., & Caruso, U. (2019). A highly efficient white luminescent zinc (II) based metallopolymer by RGB approach. *Polymers*, (10), 11. https://doi.org/10.3390/polym11101712

Pascale, F., D'Arco, P., Silvio Gentile, F., & Dovesi, R. (2022). Strategies for the optimization of the structure of crystalline compounds. *Journal of Computational Chemistry, 43*(3), 184–196. https://doi.org/10.1002/jcc.26781

Passafiume, A., Rossetti, A., Vescovi, L., Malavolti, M., Baraldi, C., Rovesti, S., … Filippini, T. (2023). Sulfur content in foods consumed in an Italian population and impact of diet quality on sulfur intake. *Journal of Food Composition and Analysis, 123*, Article 105543. https://doi.org/10.1016/j.jfca.2023.105543

Pecsok, R. L., & Juvet, R. S., Jr. (1955). The gluconate complexes. I. Copper gluconate complexes in strongly basic media1. *Journal of the American Chemical Society, 77*(1), 202–206. https://doi.org/10.1021/ja01606a076

Perez de Vargas-Sansalvador, I. M., Erenas, M. M., Martínez-Olmos, A., Mirza-Montoro, F., Diamond, D., & Capitan-Vallvey, L. F. (2020). Smartphone based meat freshness detection. *Talanta, 216*, Article 120985. https://doi.org/10.1016/j.talanta.2020.120985

Platonenko, A., Gentile, F. S., Maul, J., Pascale, F., Kotomin, E. A., & Dovesi, R. (2019). Nitrogen interstitial defects in silicon. A quantum mechanical investigation of the structural, electronic and vibrational properties. *Materials Today Communications, 21*. https://doi.org/10.1016/j.mtcomm.2019.100616

Protopappas, L., Bechtsis, D., & Tsotsolas, N. (2025). IoT services for monitoring food supply chains. *Applied Sciences (Switzerland)*, (13), 15. https://doi.org/10.3390/app15137602

Rajic, S., Đorđević, V., Tomasevic, I., & Djekic, I. (2022). The role of food systems in achieving the sustainable development goals: Environmental perspective. *Business Strategy and the Environment, 31*(3), 988–1001. https://doi.org/10.1002/bse.2930

Reis, F., Wu, S., & Potyatynnyk, K. (2017). Life in plastic, It's not fantastic: The economics of plastic pollution. *Science for Sustainability (S4S) Journal, 1*(1). https://doi.org/10.53466/VERI6053.S4SREI

Roy, S., Priyadarshi, R., Łopusiewicz, Ł., Biswas, D., Chandel, V., & Rhim, J.-W. (2023). Recent progress in pectin extraction, characterization, and pectin-based films for active food packaging applications: A review. *International Journal of Biological Macromolecules, 239*, Article 124248. https://doi.org/10.1016/j.ijbiomac.2023.124248

Sigfridsson, E., & Ryde, U. (1998). Comparison of methods for deriving atomic charges from the electrostatic potential and moments. *Journal of Computational Chemistry, 19* (4), 377–395. https://doi.org/10.1002/(SICI)1096-987X(199803)19, 4<377::AID-JCC1>3.0.CO;2-P.

Silva, R. R. A., de Freitas, P. A. V., de Oliveira, T. V., Teixeira, S. C., Rigolon, T. C. B., Stringheta, P. C., … Soares, N. D. F. F. (2024). Fraud-proof methylcellulose-based fish freshness indicator: Reversibility in halochromic sensing of basic volatiles is tailored by ionic strength. *International Journal of Biological Macromolecules*, 277. https://doi.org/10.1016/j.ijbiomac.2024.134486

Smith, R. C., Reed, V. D., & Hill, W. E. (1994). Oxidation of thiols by copper(II). *Phosphorus, Sulfur, and Silicon and the Related Elements, 90*(1-4), 147–154. https://doi.org/10.1080/10426509408016396

Stoica, M., Bichescu, C. I., Crețu, C.-M., Dragomir, M., Ivan, A. S., Podaru, G. M., … Stuparu-Crețu, M. (2024). Review of bio-based biodegradable polymers: Smart solutions for sustainable food packaging. *Foods, 13* (Vol.).

Tarkhanova, I., Gantman, M., Chizhov, A., & Smirnov, V. (2010). Conjugated oxidation of thiols and amines in the presence of copper complexes. *Reaction Kinetics, Mechanisms and Catalysis, 101*, 267–278. https://doi.org/10.1007/s11144-010-0230-y

Teymouri, Z., & Shekarchizadeh, H. (2022). A colorimetric indicator based on copper nanoparticles for volatile sulfur compounds to monitor fish spoilage in intelligent packaging. *Food Packaging and Shelf Life, 33*, Article 100884. https://doi.org/10.1016/j.fpsl.2022.100884

Tian, G., Xi, J., Yeung, M., & Ren, G. (2020). Characteristics and mechanisms of H2S production in anaerobic digestion of food waste. *Science of the Total Environment, 724*. https://doi.org/10.1016/j.scitotenv.2020.137977

Tiwari, S., Kate, A., Mohapatra, D., Tripathi, M. K., Ray, H., Akuli, A., … Modhera, B. (2020). Volatile organic compounds (VOCs): Biomarkers for quality management of horticultural commodities during storage through e-sensing. *Trends in Food Science & Technology, 106*, 417–433. https://doi.org/10.1016/j.tifs.2020.10.039

Tomasi, J., Mennucci, B., & Cammi, R. (2005). Quantum mechanical continuum solvation models. *Chemical Reviews, 105*(8), 2999–3093. https://doi.org/10.1021/cr9904009

van Haveren, J., van Bekkum, H., & Peters, J. A. (1993). The influence of pH on the coordination of copper(II) by 2-amino-2-deoxy-D-gluconate and 2-amino-2-deoxy-D-glucose oxime as studied by 1H and 13C NMR relaxation rate measurements and EPR spectroscopy. *Inorganica Chimica Acta, 205*(1), 1–7. https://doi.org/10.1016/S0020-1693(00)87347-8

Velásquez-Yévenes, L., & Ram, R. (2022). The aqueous chemistry of the copper-ammonia system and its implications for the sustainable recovery of copper. *Cleaner Engineering and Technology, 9*, Article 100515. https://doi.org/10.1016/j.clet.2022.100515

Wayman, C., & Niemann, H. (2021). The fate of plastic in the ocean environment – a minireview. *Environmental Science: Processes & Impacts, 23*(2), 198–212. https://doi.org/10.1039/D0EM00446D

Ye, P., Li, X., Xie, Y.-N., & Wu, P. (2022). Facile monitoring of meat freshness with a self-constructed photosensitization colorimetric instrument. *Food Chemistry, 385*, Article 132676. https://doi.org/10.1016/j.foodchem.2022.132676

Yin, J.-J., Fu, P. P., Lutterodt, H., Zhou, Y.-T., Antholine, W. E., & Wamer, W. (2012). Dual role of selected antioxidants found in dietary supplements: Crossover between anti- and pro-oxidant activities in the presence of copper. *Journal of Agricultural and Food Chemistry, 60*(10), 2554–2561. https://doi.org/10.1021/jf204724w

Zhao, L., Liu, Y., Zhao, L., & Wang, Y. (2022). Anthocyanin-based pH-sensitive smart packaging films for monitoring food freshness. *Journal of Agriculture and Food Research, 9*, Article 100340. https://doi.org/10.1016/j.jafr.2022.100340

Zouharová, A., Bartáková, K., Bursová, Š., Necidová, L., Haruštiaková, D., Klimešová, M., & Vorlová, L. (2023). Meat and fish packaging and its impact on the shelf life – a review. *Acta Veterinaria Brno*.